arXiv:0904.2681v1 [cond-mat.supr-con] 17 Apr 2009

Localization-delocalization dichotomy: Inherent spectral properties of the cuprates

J. Ranninger[1] and T. Domański[2]

[1]*Institut Néel, CNRS et Université Joseph Fourier, BP 166, 38042 Grenoble Cedex 09, France*
[2]*Institute of Physics, Marie Curie-Skłodowska University, 20-031 Lublin, Poland*

(Dated: April 17, 2009)

We consider hole pairing in the pseudopgap phase of High T_c cuprates, as arising from resonant scattering on dynamically deformable molecular units. As a result, localized and delocalized features coexist in the one-particle spectra: the pseudogap and propagating diffusive Bogoliubov modes. Due to the anisotropy of the electron dispersion and pairing interaction, these two manifestations have different impact in the different regions of the Brillouin zone. We illustrate that for k-vectors crossing the arc, determined by the chemical potential, joining the anti-nodal and the nodal point.

PACS numbers: 74.20.-z,74.20.Mn,74.40.+k

Introduction. - We explore the spectral features of the high T_c cuprates within a scenario of resonant pairing, which characterizes systems close to a lattice fluctuation driven Superconductor - Insulator transition (SIT). The one-particle spectra are then determined by an interplay between localization and delocalization processes which originate on molecular scale [Cu-O-Cu] bonds [1, 2]. Together with their correlated deformable ligand environments [3], they act as potential pairing centers [4] for the doped holes and break translational/rotational symmetry [5] on a finite space-time scale. Systems, prone to dynamical lattice instabilities [6], exist as metastable single phase solid solutions. Their kinetic stability is achieved by synthesization at temperatures high enough such that the entropy contribution to the free energy stabilizes misfits between different stable cation-ligand complexes [7], which are then frozen in upon solidification. In the cuprates those misfits come from an incompatibility between Cu-O distances of stable square planar [Cu-O_4] configurations in the CuO_2 planes and of cation-ligand distances in the adjacent layers.

Our contention is the following: The formal chemical Cu valence in the CuO_2 planes lies between II and III (not to be confused with the ionic charge), which corresponds to stereochemical [Cu-O] distances in the [Cu-O_4] units of 1.94 $\AA$, respectively 1.84 $\AA$. The misfits between layers leads to dynamically unstable [Cu-O_4] units, linked by a bridging O which fluctuates in and out of the CuO_2 planes. This implies fluctuations between kinked dumb-bells [Cu^{II}-O-Cu^{II}] (characteristic for the undoped systems) and straight dumb-bells [Cu^{III}-O-Cu^{III}], which capture momentarily two holes in the doped cuprates. It results in local charge/deformation fluctuations which break up the over-all homogeneous structure of the cuprates (Fig. 1 and scanning tunneling microscopy (STM) results, Figs. 4 and 5 in ref. [5]) into: (i) checkerboard charge ordered directionally oriented Cu_2O_7 domains (three nearest neighbor Cu-Cu distances wide), which act as valence fluctuating driven pairing centers and (ii) a quadratic sublattice structure composed of Cu_4 plaquettes on which the holes behave as delocalized strongly correlated entities, subject to $d_{x^2-y^2}$-wave pairing correlations [8, 9]. The local lattice fluctuations of the Cu_2O_7 domains prevent translational symmetry breaking, such that on a macroscopic level those materials exhibit an overall homogeneous crystal structure in a coarse grained sense [10]. Exceptionally ($La_{2-x}Ba_xCuO_4$ for x=1/8), local lattice deformations can lock together in a charge ordered phase, and in this way impeach a superconducting state [11]).

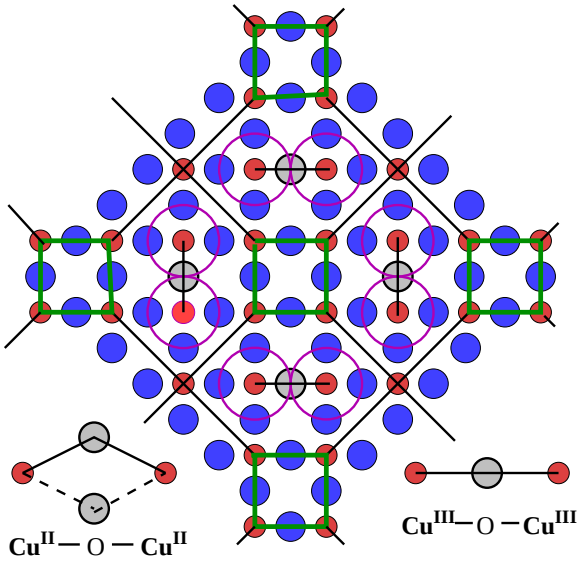

FIG. 1: (Color online) Local structure of the CuO_2 plane in form of (i) Cu_2O_7 domains acting as localizing pairing centers with directionally oriented Cu-O-Cu dumb-bells with central bridging O's (grey circles) and (ii) Cu_4 plaquettes (green square) housing the delocalized charge carriers. Small red circles denote Cu cations and the larger blue ones the O anions.

In the cuprates, resonant pairing driven by local dynamical lattice fluctuations finds its support in great a variety of experimental findings: the longitudinal optical (LO) Cu-O bond stretching mode of about 50 meV is strongly coupled to charge carriers near the *hotspot*

anti-nodal points in the Brillouin zone (BZ) $[q_x, q_y] = [\pm\pi/2, 0], [0, \pm\pi/2]$, where their pairing results in the pseudogap feature [3]. Upon entering the superconducting doping regime, coming from the insulating parent compound, this LO mode splits into two modes, separated by $\simeq$ 10 meV [12]. It indicates a crystal lattice symmetry breaking linked to dynamical charge inhomogeneities. Pressure [13], isotope substitution studies [14] and spatially resolved d^2I/dV^2-imaging [3] show concomitant (anticorrelated) modulations of the pseudo-gap size and the frequency of this LO buckling mode.

Resonant scattering of holes between the selftrapping Cu_2O_7 domains and the Cu_4 plaquettes, making up a sublattice structure, induces pairing correlations on that latter. The holes acquire (i) localized features in the high energy sector of the one-particle spectrum and (ii) delocalized low energy features of coherently propagating diamagnetic fluctuations. The first are manifest in the pseudogap phenomenon and the latter in propagating strongly bound Cooper pairs. These features derive from competing amplitude and phase fluctuations of the order parameter with energy scales k_BT^* and k_BT_c and result in the anti-correlated $T_c - T^*$ relation, as the SIT is approached upon underdoping. Sometimes, this is interpreted as describing two different energy gaps [15, 16].

Resonant scattering between itinerant fermionic charge carriers (holes or electrons) and bosonic tightly bound pairs of them near a SIT, can be accounted for by a phenomenological Boson Fermion Model (BFM). This model was originally proposed by one of us (JR) in the early eighties in an attempt to describe the relatively abrupt cross-over between a weak coupling adiabatic electron-phonon mediated BCS superconductor and an insulating state of diffusive bipolarons in the strong coupling anti-adiabatic regime. The BFM describes itinerant fermions in chemical equilibrium with localized bound pairs (bipolarons) of them. It captures a situation of a single-component system, where at any given moment a certain percentage of the charge carriers is locally paired [6]. The superconducting, respectively insulating gap in such a system is centered at the chemical potential and determines the Fermi surface, which may be hidden. The opening of this gap does not depend on a particular set of Fermi wavevectors and hence is unrelated to any global translational symmetry breaking. The insulating state is a Mott correlation driven phase of singlet-*bonding pairs* [17, 18]. To what extent such a phase fluctuation driven insulator could result in a Cooper-pair Wigner crystal, had been examined [19, 20]. It predicted a texturing coming from vortex-antivortex fluctuations rather than from the local lattice instabilities we evoke here.

The anisotropy of pairing and of the hole dispersion in the CuO_2 planes marks the relative importance of localization versus delocalization of the charge carriers. This is clearly manifest, as we move along the arc in the BZ, which corresponds to the Fermi surface in the non-interacting system. Near the anti-nodal points strong pairing results from strong intra-*bonding pair* phase correlations between bound fermion pairs and their itinerant counterparts [21, 22]. It leads to localization, which shows up in form of a pseudogap in the one-particle spectral properties and destroys the Fermi surface. As one moves toward the nodal points, $[k_x, k_y] = [\pm\pi/2, \pm\pi/2]$, the intra-*bonding pair* phase correlations are weakened. It results in increased amplitude fluctuations and hence a reduction of the degree of localization, manifest in a reduced size of the pseudogap. At the same time, upon approaching the nodal points, the inter-*bonding pair* phase correlations are strengthened and with it the spatial superconducting phase locking. This leads to Bogoliubov modes, which emerge out of localized phase uncorrelated singlet-*bonding* and *anti-bonding pairs*. We derive below these properties on the basis of the BFM, adapted to the specific anisotropic features of the cuprates.

The Model. - The salient feature of the BFM is a charge exchange term which controls the transfer of electrons (holes) between real and momentum space [23].

$$H^{exch}_{BFM} = \frac{1}{\sqrt{N}} \sum_{\mathbf{k},\mathbf{q}} (g_{\mathbf{k},\mathbf{q}} b^\dagger_{\mathbf{q}} c_{\mathbf{q}-\mathbf{k},\downarrow} c_{\mathbf{k},\uparrow} + H.c.). \quad (1)$$

It comprises localized bound electron (hole) singlet pairs ($b^{(\dagger)}_{\mathbf{q}}$) and their itinerant counterparts, i.e., fermionic charge carriers ($c^{(\dagger)}_{\mathbf{k}\sigma}$), located respectively on the deformable Cu_2O_7 domains and the Cu_4 plaquettes. We shall here consider effective sites, centered at the quadratic Cu_4 plaquettes and which include the surrounding Cu_2O_7 domains. The effective BFM Hamiltonian for such a scenario then is: $H_{BFM} = H^0_{BFM} + H^{exch}_{BFM}$, where

$$H^0_{BFM} = \sum_{\mathbf{k}} (\varepsilon_{\mathbf{k}} - \mu) c^\dagger_{\mathbf{k}} c_{\mathbf{k}} + \sum_{\mathbf{q}} (E_{\mathbf{q}} - 2\mu) b^\dagger_{\mathbf{q}} b_{\mathbf{q}}. \quad (2)$$

The bare dispersion of the fermions and the intrinsically localized bosons is $\varepsilon_k = \varepsilon^0_k$, respectively $E_{\mathbf{q}} = 2\Delta$. The single component nature of such systems is enforced by a unique chemical potential μ. We assume the standard anisotropic bare electron dispersion of the CuO_2 planes as $\varepsilon^0_{\mathbf{k}} = -2t[cosk_x + cosk_y] + 4t' cosk_x cosk_y$ with $t'/t = 0.4$ and an anisotropic bare d-wave exchange coupling $g^0_{\mathbf{k},\mathbf{q}} = g[cosk_x - cosk_y]\delta_{q,0}$. The interplay between the delocalizing and the localizing effect is described by H^{exch}_{BFM}. It results in a competition between local intra-pair correlations leading to an insulator and spatial inter-pair correlations leading to a superconductor, as the strength of the exchange coupling $g^0_{\mathbf{k},\mathbf{q}}$ decreases. Close to the SIT, the fermionic features have strong contributions coming from the bosonic particles and vice versa. Our aim therefore is to reformulate this interacting Boson-Fermion mixture in terms of two effective commuting Hamiltonians, one describing purely fermionic excitations and one purely bosonic ones. The boson-fermion

interaction thereby is absorbed into interdependent coupling constants by renormalizing $g_{\mathbf{k},\mathbf{q}}$ down to zero via a flow-equation renormalization procedure [24, 25]. For isotropic exchange coupling and fermion dispersions this problem has been studied previously [18, 26, 27], predicting the pseudogap [28] and damped Bogoliubov modes [27] in angle resolved photoemission spectra. Both have since been verified experimentally [29].

Localization versus delocalization. - We now illustrate how the specific anisotropic pairing and dispersion in the cuprate CuO_2 planes influence the spectral properties as one moves along the arc in the BZ, mentioned above. The flow equation technique projects at every step of this procedure the renormalized Hamiltonian onto the basic structure given by H^0_{BFM} in eq. 2 plus renormalization induced fermion-fermion interactions $U_{\mathbf{k},\mathbf{p}}$ [26]. In this way, the various parameters $\varepsilon_{\mathbf{k}}(\ell), E_{\mathbf{q}}(\ell), g_{\mathbf{k},\mathbf{q}}(\ell), \mu(\ell)$, characterizing H^0 and H_{exch} evolve as the flow parameter ℓ increases. The renormalization procedure starts with parameters corresponding to $\ell = 0$, given by $\varepsilon^0_{\mathbf{k}}, 2\Delta$ and $g^0_{\mathbf{k},0}$. The chemical potential $\mu(\ell)$ is chosen at each step of the renormalization flow such as to fix a given total number of fermions and bosons. As a representative example we take $n_{tot} = \sum_\sigma n^F_\sigma + 2n^B = 1$, such as to reproduce the appropriate size and shape of the CuO_2 plane Fermi surface. We concentrate on the spectral functions for electrons with wave vectors $\mathbf{k} = |\mathbf{k}|[sin\phi, cos\phi]$, orthogonally intersecting the arc at various $\mathbf{k}_F$, where the motion of the holes is essentially one dimensional. ϕ denotes the angle of those $\mathbf{k}$-vectors with respect to the line $[\pi,\pi] - [\pi, 0]$ (see Fig.3).

The renormalization procedure consists of transforming the Hamiltonian in infinitesimal steps, controlled by the differential equation $\partial_\ell H(\ell) = [\eta(\ell), H(\ell)]$. In its canonical form [24], $\eta(\ell) = [H_0(\ell), H(\ell)]$ is an anti-Hermitean generator. For details of the ensuing coupled non-linear differential equations for the various ℓ dependent parameters, we refer the reader to our previous work [26, 27]. The flow of these parameters converges for $\ell \to \infty$ and results in two uncoupled systems: one for the fermionic excitations and one for the bosonic ones with a fixed point Fermion dispersion $\varepsilon^*_{\mathbf{k}} = \varepsilon_{\mathbf{k}}(\ell \to \infty)$. The bare exchange coupling $g^0_{\mathbf{k},0}$, being equal to zero at the nodal point ($\phi = \pi/4$), steadily increases as one moves to the anti-nodal point ($\phi = 0$), where it achieves its maximal value, equal to g. As a consequence, $\varepsilon^*_{\mathbf{k}}$ remains essentially unrenormalized for $\mathbf{k}$ vectors crossing the arc near the nodal point. Upon approaching the anti-nodal point, on the contrary, it acquires an S-like inflexion at $\mathbf{k}_F$. Upon reducing the temperature T, it becomes increasingly more pronounced and foreshadows the evolution into a true superconducting gap below T_c.

In order to obtain the renormalized spectral function for the charge carriers, a similar renormalization procedure is applied to the fermion and boson operators. Their

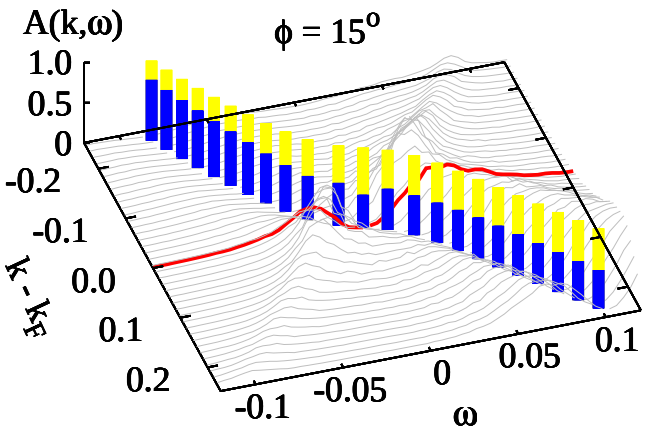

FIG. 2: (Color online) $A(\mathbf{k},\omega)$ at $T = 0.007$ ($< T^* = 0.016$) as a function of $|\mathbf{k}|$ (in units of the inverse lattice vector) near $\mathbf{k}_F$ (red line), corresponding to $\phi = 15^o$, orthogonally crossing the arc. The spectral weight of the coherent and incoherent contributions are indicated by blue, respectively yellow bars.

effective structure is given by [27]

$$\begin{bmatrix} c^\dagger_{-\mathbf{k},-\sigma}(\ell) \\ c_{\mathbf{k},\sigma}(\ell) \end{bmatrix} = u_{\mathbf{k}}(\ell) \begin{bmatrix} c^\dagger_{-\mathbf{k},-\sigma} \\ c_{\mathbf{k},\sigma} \end{bmatrix} \mp \frac{1}{\sqrt{N}} \sum_{\mathbf{q}} v_{\mathbf{k},\mathbf{q}}(\ell) \begin{bmatrix} b^\dagger_{\mathbf{q}} c_{\mathbf{q}+\mathbf{k},\sigma} \\ b_{\mathbf{q}} c^\dagger_{\mathbf{q}-\mathbf{k},-\sigma} \end{bmatrix} \tag{3}$$

The ℓ dependent parameters $u_{\mathbf{k}}(\ell), v_{\mathbf{k}}(\ell)$ are determined by corresponding flow equations and result in a fermionic spectral function of the form

$$A(\mathbf{k},\omega) = |u^*_{\mathbf{k}}|^2 \delta(\omega + \mu - \varepsilon^*_{\mathbf{k}}) + \frac{1}{N} \sum_{\mathbf{q}\neq\mathbf{0}} \left(n^B_{\mathbf{q}} + n^F_{\mathbf{q}-\mathbf{k}\downarrow}\right) |v^*_{\mathbf{k},\mathbf{q}}|^2 \delta(\omega - \mu + \varepsilon^*_{\mathbf{q}-\mathbf{k}} - E^*_{\mathbf{q}}), \tag{4}$$

We illustrate in Fig.2 this spectral function for a characteristic region on the arc (corresponding to $\phi = 15^o$), separating the localization from the delocalization dominated regime for g = 0.1 and $\Delta = 0.075$ in units of a nominal band width $D = 8t$. For $|\mathbf{k}| < |\mathbf{k}|_F$ it consists of essentially delocalized features (the first term) following the dispersion $\varepsilon^*_{\mathbf{k}}$. For $|\mathbf{k}|_F < |\mathbf{k}| < |\mathbf{k}|_0$, in a corresponding energy interval $[\varepsilon_F, \varepsilon_F + \sqrt{\Delta^2 + Zg^2}]$, the delocalized features, given by $\varepsilon^*_{\mathbf{k}}$, are accompanied by localized ones (the second term). They reflect diffusively propagating images of localized bonding and anti-bonding states, such as given by the Green's function in the atomic limit $(t, t' = 0)$ [21, 22], $G(i\omega_n) = 1/[G^0(i\omega_n)^{-1} - \Sigma(i\omega_n)]$ with

$$\Sigma(i\omega_n) = \frac{(1-Z)\, g^2\, (i\omega_n + \mu)}{[(i\omega_n + \mu)(i\omega_n - 2\Delta + \mu) - Zg^2]}, \tag{5}$$

having the structure of a BCS self-energy for localized Cooper pairs. $Z \simeq 2/[3 + \cosh(g/k_BT)]$ (for our choice of parameters) denotes the spectral weight of

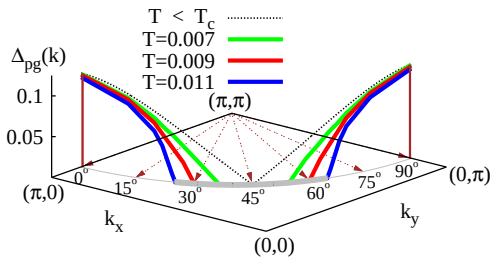

FIG. 3: (Color online) Variation of the pseudogap for different k vectors, orthogonally crossing the arc, given by angles ϕ.

non-bonding delocalized charge carriers, described by $G^0(i\omega_n) = 1/(i\omega_n - \mu)$. In the normal state (constituted of an ensemble of spatially phase uncorrelated diffusively propagating *bonding* pairs) this atomic limit spectral feature dictates (i) a broadened lower Bogoliubov band for $|\mathbf{k}| > |\mathbf{k}|_F$ and (ii) a broadened upper Bogoliubov band for $|\mathbf{k}| < |\mathbf{k}|_F$, extending down to $k = 0$, where it merges into the time reversed spectrum $-\varepsilon^*_{\mathbf{k}}$. A pseudogap gap in the partial density of states, $\rho(\omega) = (1/N)\sum_{|\mathbf{k}|} A(\mathbf{k},\omega)$ opens up at some $T = T^*$ at $\mathbf{k}_F$. Its size, Δ_{pg}, is determined by the distance between the peaks around $\varepsilon^*_{\mathbf{k}_F}$, when upon lowering T the deviation from the bare density of state, $\rho^0(\omega) = (1/N)\sum_{|\mathbf{k}|}\delta(\omega - \varepsilon_{\mathbf{k}})$ is reduced by 90%. These features are attenuated, respectively enhanced, when we move along the arc toward the nodal, respectively the antinodal, points. We illustrate in Fig. 3. the variation of Δ_{pg} for different T. Close to the antinodal point - the localization dominated regime - it is relatively T independent. But approaching the nodal point it abruptly drops to zero, already for finite values of $g^0_{\mathbf{k},0}$, which lets us envisage a BCS like onset of superconductivity (without any pseudogap) for $60^o \geq \phi \geq 30^o$. Close to $\mathbf{k}_F$ the effect of fermion-fermion interaction $U_{\mathbf{k},\mathbf{p}}$ is expected to change the poles of the coherent contributions into cut-singularities with complex residues, effectively showing up in $A(\mathbf{k},\omega)$ as broad peaks [28, 30]. This effect of $U_{\mathbf{k},\mathbf{p}}$ could possibly result in a second gap [15, 16], inside the rather T insensitive pseudogap, albeit that latter persisting into the superconducting phase upon lowering T. Concerning the evolution of the pseudogap phase into either a superconducting or insulating one, we have to understand how these various parts of the BZ with dominating localizing, respectively delocalizing, effects are connected [31]. This will depend on the conditions under which the bosonic charge carriers condense into either a phase correlated or phase uncorrelated state. These questions will be addressed in future.

Summary.-The present scenario for the cuprates is based on resonant pairing, induced by local dynamical lattice instabilities. It makes use of the fact that such systems are prone to segmentations which implies charge carriers existing simultaneously in (i) quasi localized states, originating from polaronic self-trapping in valence fluctuating local domains and (ii) delocalized states on a sublattice in which those domains are embedded. This scenario implies pairing correlations of varying strength in different regions of the BZ - a feature which had been conjectured [32] early on, trying to avoid the stringent limitations of T_c within a BCS scenario.

[1] Y. Kohsaka et al., Science **315**, 1380 (2007).
[2] K. K. Gomes et al., Nature **447**, (2007).
[3] Y. Lee et al., Nature **442**, 546 (2006).
[4] K. McElroy et al., Nature bf 442, 592 (2003).
[5] Y. Kohsaka et al., Nature **454**, 1072 (2008).
[6] J. Ranninger and A. Romano, Phys. Rev. B **78**, 054527 (2008).
[7] A. W. Sleight, Physics Today, **44**(6), 24 (1991).
[8] J. E. Hirsch, S. Tang, E. Loh, Jr. and D. J. Scalapino, Phys. Rev. Lett. **60**, 1668 (1988).
[9] E. Altman and A. Auerbach, Phys. Rev. B **65**, 104508 (2002).
[10] A. V. Balatsky and J.-X. Zhu, Phys. Rev. B **74**, 094517 (2006).
[11] T. Valla et al., Science **314**, 914 (2006).
[12] D. Reznik et al., Nature **440**, 1170 (2006).
[13] P. S. Haeflinger et al., Europhys. Lett. **73**, 260 (2006).
[14] D. Rubio Temprano et al., Phys. Rev. Lett. **84**, 1990 (2000).
[15] Z. Tesanovic, Nature Phys. **4**, 408 (2008).
[16] S. Huefner et al., Rep. Prog. Phys. **71**, 062501 (2008).
[17] M. Cuoco and J. Ranninger, Phys. Rev. B **74**, 094511 (2006)
[18] T. Stauber and J. Ranninger, Phys. Rev. Lett. **99**, 045301 (2007).
[19] Z. Tesanovic, Phys. Rev. Lett. **93**, 217004 (2004).
[20] T. Pereg-Barnea and M. Franz, Phys. Rev.B **74**, 014518 (2006).
[21] T. Domanski, J. Ranninger and J. M. Robin, Solid State Commun. **96**, 559 (1996).
[22] T. Domanski, Eur. Phys. J. B **33**, 41 (2003).
[23] T. Hanaguri, Nature **454**, 1062 (2008).
[24] F. Wegner, Ann. Phys. (Leipzig) **3**,77 (1994).
[25] S. D. Glazek and K. G. Wilson, Phys. Rev. D **48**, 5863 (1993).
[26] T. Domanski and J. Ranninger, Phys. Rev. B **63** 134505 (2001).
[27] T. Domanski and J. Ranninger, Phys. Rev. Lett. **91**, 255301 (2003).
[28] J. Ranninger, J. M. Robin and M. Eschrig, Phys. Rev. Lett. **74**, 4027 (1995).
[29] A. G. Loeser et al., Science **273**, 325 (1996); H. Ding et al., Nature **382**, 51 (1996); A. Kanigel et al., Phys. Rev. Lett. **101**, 137002 (2008).
[30] J. Ranninger and J. M. Robin, Solid State Commun., **105**, 473 (1996).
[31] A. Perali et al., Phys. Rev. B **62**, R9295 (2000).
[32] P. W. Anderson, Science **144**, 373 (1964).